Received: 4 September 2020 | Revised: 18 August 2021 | Accepted: 4 September 2021

DOI: 10.1002/1348-9585.12282

Journal of Occupational Health Open Access WILEY

ORIGINAL ARTICLE

MicroRNA expression in lung tissues of asbestos-exposed mice: Upregulation of miR-21 and downregulation of tumor suppressor genes *Pdcd4* and *Reck*

Yusuke Hiraku[1,2] | **Jun Watanabe**[2] | **Akira Kaneko**[2] | **Takamichi Ichinose**[3] | **Mariko Murata**[2]

[1]Department of Environmental Health, University of Fukui School of Medical Sciences, Eiheiji, Fukui, Japan

[2]Department of Environmental and Molecular Medicine, Mie University Graduate School of Medicine, Tsu, Mie, Japan

[3]Department of Health Sciences, Oita University of Nursing and Health Sciences, Oita, Japan

Correspondence
Yusuke Hiraku, Department of Environmental Health, University of Fukui School of Medical Sciences, 23-3 Matsuoka Shimoaizuki, Eiheiji, Fukui 910-1193, Japan.
Email: y-hiraku@u-fukui.ac.jp

Funding information
Ministry of Education, Culture, Sports, Science and Technology, Japan, Grant/Award Number: 23659328 : 24390153, 15H04784 and 18H03038; Grants-in-Aid for Scientific Research

Abstract

Objectives: Asbestos causes lung cancer and malignant mesothelioma in humans, but the precise mechanism has not been well understood. MicroRNA (miRNA) is a short non-coding RNA that suppresses gene expression and participates in human diseases including cancer. In this study, we examined the expression levels of miRNA and potential target genes in lung tissues of asbestos-exposed mice by microarray analysis.

Methods: We intratracheally administered asbestos (chrysotile and crocidolite, 0.05 or 0.2 mg/instillation) to 6-week-old ICR male mice four times weekly. We extracted total RNA from lung tissues and performed microarray analysis for miRNA and gene expression. We also carried out real-time polymerase chain reaction (PCR), Western blotting, and immunohistochemistry to confirm the results of microarray analysis.

Results: Microarray analysis revealed that the expression levels of 14 miRNAs were significantly changed by chrysotile and/or crocidolite (>2-fold, $P < .05$). Especially, miR-21, an oncogenic miRNA, was significantly upregulated by both chrysotile and crocidolite. In database analysis, miR-21 was predicted to target tumor suppressor genes programmed cell death 4 (*Pdcd4*) and reversion-inducing-cysteine-rich protein with kazal motifs (*Reck*). Although real-time PCR showed that *Pdcd4* was not significantly downregulated by asbestos exposure, Western blotting and immunohistochemistry revealed that PDCD4 expression was reduced especially by chrysotile. *Reck* was significantly downregulated by chrysotile in real-time PCR and immunohistochemistry.

Conclusions: This is the first study demonstrating that miR-21 was upregulated and corresponding tumor suppressor genes were downregulated in lung tissues of asbestos-exposed animals. These molecular events are considered to be an early response to asbestos exposure and may contribute to pulmonary toxicity and carcinogenesis.

KEYWORDS
asbestos, cancer, lung, microRNA, *Pdcd4*, *Reck*

1 | INTRODUCTION

Asbestos is a naturally occurring fiber that has been used for a various industrial purposes, and causes lung cancer and malignant mesothelioma of the pleura and peritoneum. The International Agency for Research on Cancer (IARC) has evaluated asbestos to be carcinogenic to humans (Group 1).[1] Although asbestos use has been banned in developed countries and estimated worldwide asbestos consumption has recently been decreased, in some regions of the world, asbestos production has remained steady because of its continued demand.[2] Therefore, there is a serious concern that the cases of asbestos-related diseases will increase especially in developing countries. However, the precise mechanism of asbestos-induced carcinogenesis has not been understood. Several possible mechanisms for asbestos-induced carcinogenesis, such as irritation of the pleura, mitosis disruption via interaction with mitotic spindle, generation of reactive oxygen species, and activation of signaling pathways leading to upregulation of protooncogenes, have been proposed.[3] We have previously reported that subacute intratracheal exposure to asbestos fibers induced the formation of 8-nitroguanine, a nitrative DNA lesion formed during inflammation, in lung tissues of mice.[4] In human lung tissues, the extent of 8-nitroguanine formation was significantly correlated with asbestos fiber content.[5]

Regarding molecular events involved in environmental carcinogenesis, not only genetic changes but also epigenetic changes, including DNA methylation, histone modification, and alteration in microRNA (miRNA) expression, are considered to play a substantial role. miRNA is a small non-coding RNA that binds to messenger RNA (mRNA) of the target genes to suppress their expression. Alteration in the expression level of miRNA contributes to various human diseases including cancer. miRNA is expected to be a potential biomarker of asbestos-induced malignancies.[6,7] In relation to asbestos exposure, the expression pattern of miRNA was investigated in human malignant mesothelioma tissues, and several miRNAs were differentially expressed in mesothelioma and normal tissues[8] and different histopathological subtypes.[9] Several studies have reported different abundance of several miRNAs in plasma between mesothelioma patients and non-cancerous control subjects.[10–12] A recent animal study has demonstrated that several miRNAs are overexpressed in asbestos-induced rat sarcomatoid mesothelioma.[13] However, the role of miRNA in the pathogenesis of asbestos-induced carcinogenesis is not well understood. In addition, the expression pattern of miRNA and predicted target genes has not been investigated in lung tissues of asbestos-exposed animals. Asbestos fibers are classified as serpentine (chrysotile) and amphibole (crocidolite, amosite and others), but the difference in miRNA profile in lung tissues of animals exposed to different types of asbestos has not been investigated.

In this study, we examined miRNA and gene expression in lung tissues of asbestos-exposed mice by microarray analysis. We employed a mouse model of subacute asbestos exposure to examine miRNA expression as an early response leading to pulmonary toxicity and carcinogenicity. We performed database analysis to predict target genes of miRNA that was differentially expressed in asbestos-exposed mice. We validated the expression of miRNA and predicted target genes by real-time polymerase chain reaction (PCR), Western blotting and immunohistochemistry. Especially, miR-21 is known to be an oncogenic miRNA that was upregulated in human lung cancer tissues compared with normal tissues[14] and targets tumor suppressor genes, including programmed cell death 4 (*Pdcd4*) and reversion-inducing-cysteine-rich protein with kazal motifs (*Reck*).[15,16] In this study, according to our results, we focused on upregulation of miR-21 and downregulation of tumor suppressor genes in relation to asbestos-induced carcinogenesis.

2 | MATERIALS AND METHODS

2.1 | Animal experiments

ICR male mice (6 weeks of age, Japan Clea) were housed in plastic cages lined with soft wood chips. The cages were placed in a conventional room, which was air-conditioned at 23℃ and 55%–70% humidity with a light/dark (12 h/12 h) cycle. Mice were given a commercial diet and water *ad libitum*. Asbestos fibers used in this study were standard reference samples of Union Internationale Contre le Cancer (UICC) [chrysotile B (2.6 ± 2.3 μm of length and 0.15 ± 1.8 μm of diameter) and crocidolite (2.5 ± 2.0 μm of length and 0.33 ± 2.1 μm of diameter), mean ± standard deviation (SD)].[17] We suspended asbestos fibers in saline containing 0.05% (v/v) Tween 80 (vehicle) and then sonicated for 5 min with an ultrasonic disrupter (UD-201; Tomy) under cooling condition. Each mouse was intratracheally instilled with 0.05 mg (low dose) or 0.2 mg (high dose) of asbestos under anesthesia with 4% halothane. The instillation was repeated

four times at weekly intervals (total asbestos doses were 0.2 and 0.8 mg for low and high doses, respectively). The control mice administered the vehicle alone. We employed these experimental conditions, because we have previously demonstrated that asbestos exposure induced significant nitrative DNA damage, an initial event of carcinogenesis, under the same conditions.[4] One day after the last administration, all mice were sacrificed by exsanguination under deep anesthesia, and lung tissues were removed and stored at −80℃. The study adhered to the U.S. National Institutes of Health guidelines for the use of experimental animals. The animal care method was approved by the Animal Care and Use Committee at Oita University of Nursing and Health Sciences in Oita, Japan.

2.2 | Microarray analysis for miRNA expression

The lung tissues were obtained from asbestos-exposed mice (0.05 mg/instillation) and preserved in RNA*later*-ICE (Ambion) at −20℃. Then the tissues were homogenized in Lysis/Binding Buffer included in a *mir*Vana miRNA Isolation Kit (Ambion) using a μT-01 Beads Crusher (Taitec). Total RNA was extracted from the homogenates with this kit following the manufacturer's instructions and quantified with a BioSpec-nano UV-VIS spectrophotometer (Shimadzu). RNA (100 ng) was labeled with fluorescent cyanine 3-CTP (Cy3), included in a miRNA Complete Labeling Reagent and Hyb Kit (Agilent Technologies), following the manufacturer's instructions. Then Cy3-labeled RNA was hybridized onto a SurePrint G3 Mouse miRNA microarray (Rel. 19.0; Agilent Technologies) at 55℃ for 20 h. Hybridized microarray slides were scanned with a DNA Microarray Scanner (Agilent Technologies). The scanned images were analyzed numerically using a Feature Extraction software (version 10.7; Agilent Technologies).

2.3 | Microarray analysis for gene expression

Total RNA was extracted from the lung tissues and quantified as described above. RNA (25 ng) was reverse-transcribed to cDNA and then cRNA was synthesized and labeled with Cy3 using a Low Input Quick Amp Labeling Kit (Agilent Technologies) according to the manufacturer's instructions. Then Cy3-labeled RNA (600 ng) was hybridized onto SurePrint G3 Mouse GE microarrays (Agilent Technologies) at 65℃ for 17 h. Hybridized microarray slides were scanned and the scanned images were analyzed numerically as described above.

2.4 | Microarray data analysis

Microarray data for miRNA and gene expression were statistically analyzed with a GeneSpring GX software (version 12; Agilent Technologies). The data were normalized by 75% percentile shift as described previously.[18] We performed analysis of variance (ANOVA) followed by Tukey's test to identify differentially expressed miRNAs and genes with >2-fold change between the control and asbestos-exposed mice. P values < .05 were considered as statistically significant. We predicted target genes of these miRNAs according to the following criteria: (a) potential target genes are listed in all of the following databases: miRanda, TargetScan (Release 7.0) and PicTar; (b) expression levels were significantly changed by asbestos compared with the control (>2-fold, $P < .05$ by one-way ANOVA + Tukey's test); (c) expression levels were inversely changed from the corresponding miRNA.

2.5 | Real-time PCR for miRNA expression

To validate the expression levels of miRNAs in lung tissues of asbestos-exposed mice, we performed quantitative real-time PCR. Total RNA was extracted from lung tissues of asbestos-exposed mice with a *mir*Vana miRNA Isolation Kit (Ambion) and quantified with a BioSpec-nano UV-VIS spectrophotometer (Shimadzu). miRNA was reverse-transcribed with a TaqMan® MicroRNA Reverse Transcription Kit (Applied Biosystems). Relative miRNA expression was quantified with a StepOne Real-Time PCR System using TaqMan MicroRNA Assays (Applied Biosystems). The PCR cycling conditions were 50℃ for 2 min, 95℃ for 10 min, and 40 cycles of 95℃ for 15 s and 60℃ for 1 min. miRNA levels were normalized against the corresponding levels of U6 snRNA. Relative expression levels were calculated using the ΔΔCt method. The experiments were performed in duplicate in separate wells.

2.6 | Real-time PCR for target gene expression

To validate the expression levels of potential target genes of miRNAs, we performed real-time PCR. Total RNA was extracted from lung tissues of asbestos-exposed mice and quantified as described above. RNA was reverse-transcribed into cDNA with a High Capacity RNA-to-cDNA kit (Applied Biosystems). Relative mRNA expression was quantified with a StepOne Real-Time PCR System using TaqMan Gene Expression Assays (Applied

Biosystems). The PCR cycling conditions were 50℃ for 2 min, 95℃ for 10 min, and 40 cycles of 95℃ for 15 s and 60℃ for 1 min. mRNA levels were normalized against the corresponding levels of *Gapdh*. Relative expression levels were calculated using the ΔΔCt method. The experiments were performed in duplicate in separate wells.

2.7 | Western blotting

We quantified the expression level of PDCD4 as a potential target gene of miR-21 by Western blotting by the method described previously.[19] The lung tissues were homogenized in phosphate-buffered saline containing proteinase inhibitor cocktail (Complete Mini; Roche Diagnostics) with a μT-01 Beads Crusher (Taitec). The homogenate was centrifuged at 14 000 *g* for 10 min at 4℃, and the supernatant was used for the experiment. Protein concentration was measured using a Coomassie Protein Assay Reagent Kit (Pierce Biotechnology) following the manufacturer's instructions. Proteins were solubilized in sample buffer [2% (w/v) sodium dodecyl sulfate (SDS), 10% (v/v) glycerol, 5% (v/v) 2-mercaptoethanol, 0.001% (w/v) bromophenol blue and 50 mM Tris-HCl (pH 6.8)] and boiled for 5 min. The proteins were separated by 5%–20% SDS-polyacrylamide gel electrophoresis and blotted onto a polyvinylidene difluoride membrane, which was then treated with 5% (w/v) skim milk in Tris-buffered saline (pH 7.4) containing 0.1% (v/v) Tween 20. The membrane was incubated with rabbit polyclonal anti-PDCD4 (ab51495, 1:2000; Abcam) or anti-GAPDH (sc-25778, 1:1000, an internal standard; Santa Cruz Biotechnology) antibody for 60 min, and then with horseradish peroxidase-conjugated donkey anti-rabbit immunoglobulin G (IgG) antibody (1:2000; Santa Cruz Biotechnology) for 30 min. The membrane was treated with ECL plus Western blotting detection reagents (GE Healthcare) and analyzed with a LAS-4000 mini biomolecular imager (Fujifilm). We performed quantitative image analysis by measuring the band intensity with an ImageJ software and normalized with GAPDH.

2.8 | Histological staining and immunohistochemical analysis

To observe histopathological changes in lung tissues of asbestos-exposed mice, we performed hematoxylin and eosin (HE) staining. Fibrotic changes in the lung tissues were evaluated by Masson's trichrome (MT) staining using a Trichrome Stain Kit (ScyTek Labolatories) and aniline blue (Fujifilm Wako Pure Chemical Corporation). To examine macrophage infiltration, we performed immunoperoxidase staining for CD68, a macrophage marker, according to the method described previously.[5] Paraffin sections of lung tissues were deparaffinized, microwaved and incubated with anti-CD68 rabbit polyclonal antibody (1.5 μg/ml, ab125212; Abcam) overnight at room temperature. Then the sections were incubated with horseradish peroxidase-conjugated mouse anti-rabbit IgG antibody (sc-2357, 1:100; Santa Cruz Biotechnology) for 2 h. The immunostaining was developed by using 3,3′-diaminobenzidine tetrahydrochloride (Dojindo Laboratories) and hydrogen peroxide. The sections were counterstained with hematoxylin and observed under a light microscope.

To examine the localization and expression levels of PDCD4 and RECK in lung tissues of asbestos-exposed mice, we performed fluorescent immunohistochemical analysis as described previously.[5] Deparaffinized lung tissue sections were incubated with rabbit polyclonal anti-PDCD4 (1:100; Abcam) or anti-RECK (sc-28918, 1:200; Santa Cruz Biotechnology) antibody overnight at room temperature. Then, the sections were incubated with Alexa 594-labeled goat antibody against rabbit IgG (1:400; Molecular Probes) for 3 h. The nuclei were stained with 4′,6-diamidino-2-phenylindole contained in SlowFade Diamond (Molecular Probes). The stained sections were examined under a fluorescent microscope (BX53, Olympus). The staining intensity of each sample was quantitatively analyzed with an ImageJ software by analyzing five randomly selected fields. The proportion of positively stained cells was calculated by counting 300 cells per sample.

2.9 | Statistical analysis

For statistical analysis of the data, ANOVA followed by Tukey's test was used at a significance level of 0.05. The statistical analysis was performed by SPSS 20.0 software for Macintosh. The data represent means ± SD.

3 | RESULTS

3.1 | Differentially expressed miRNAs in lung tissues of asbestos-exposed mice

We examined miRNA expression in lung tissues of asbestos-exposed mice by microarray analysis. The expression levels of 14 miRNAs were significantly changed (>2-fold and $P < .05$, ANOVA + Tukey's test) by exposure to chrysotile and/or crocidolite compared with the control as listed in Table 1. The expression levels of four miRNAs (miR-21, miR-146b, miR-449a, and miR-486) were significantly changed by both chrysotile and crocidolite. The expression levels of nine miRNAs (miR-133a, miR-133b,

miR-144, miR-150, miR-322, miR-376b, miR-451, miR-709, and miR-1895) were significantly changed (>2-fold) by only chrysotile and one miRNA (miR-128) was significantly upregulated by only crocidolite.

3.2 | Prediction of target genes of miRNAs

We examined gene expression in lung tissues of asbestos-exposed mice by microarray analysis. In lung tissues of chrysotile- and crocidolite-exposed mice, 921 genes (569 upregulated and 352 downregulated genes), and 473 genes (206 upregulated and 267 downregulated genes) were differentially expressed (>2-fold, $P < .05$ by ANOVA + Tukey's test) compared with the control, respectively. We performed database analysis using miRanda, TargetScan and Pictar, and listed predicted target genes of corresponding miRNAs in Table 1. Predicted target genes were found for miR-21, miR-133a, miR-144, and miR-449a. The expression levels of the predicted target genes analyzed by microarray analysis are shown in Table 2. Especially, miR-21 was predicted to target *Pdcd4* and *Reck* tumor suppressor genes, and miR-133a was predicted to target glial cell line-derived neurotrophic factor (*Gdnf*), which is a ligand for the RET oncogene product.

3.3 | miRNA expression evaluated by real-time PCR

We performed real-time PCR to validate the expression levels of miR-21 and miR-133a, because they were predicted to target genes involved in tumor suppression and development, respectively. The results are shown in Figure 1. The expression level of miR-21 was significantly increased by both chrysotile and crocidolite ($P < .05$). At the high dose, the expression level of miR-21 was significantly higher in chrysotile-exposed mice than in crocidolite-exposed mice ($P < .05$). miR-133a was significantly downregulated by chrysotile exposure ($P < .01$) but crocidolite did not induce a significant change. There was a significant difference in miR-133a expression level between chrysotile- and crocidolite-exposed mice at the low dose ($P < .001$).

3.4 | Expression of predicted target genes evaluated by real-time PCR and correlation with miRNA expression

We performed real-time PCR to validate the expression levels of predicted target genes of above-mentioned miRNAs (*Pdcd4*, *Reck*, and *Gdnf*), which are known to

TABLE 1 miRNAs differentially expressed in lung tissues of asbestos-exposed mice in microarray analysis and predicted target genes

miRNA	*P*(ANOVA)	Chrysotile (fold vs. control)	Crocidolite (fold vs. control)	Predicted target genes[¶]
miR-21	.0002	3.76*	2.47*	*Pdcd4*, *Reck*
miR-146b	.0001	3.60*	2.42*	
miR-449a	<.0001	9.34*	3.85*#	*Lef1*
miR-486	.0014	−2.93*	−2.39*	
miR-133a	.0041	−71.23*	2.49#	*Gdnf*, *Ppfia3*
miR-133b	<.0001	−246.69*	−1.25#	
miR-144	.0026	−2.10*	−1.64$	*Fosb*, *Myo1e*, *Phlda1*
miR-150	.0024	−48.34*	−1.55#	
miR-322†	.0059	2.04*	1.57	
miR-376b	.0157	145.23*	−1.41#	
miR-451	.0006	−2.01*	−1.44$#	
miR-709†	.0005	2.27*	1.09#	
miR−1895†	.0108	2.04*	1.14#	
miR-128	.0025	−2.59	28.89*#	

Abbreviations: ANOVA, analysis of variance; miRNA, microRNA.

[¶] Listed in all of miRanda, TargetScan, and PicTar as potential target genes of the corresponding miRNA.

† Does not exist in humans, according to miRBase (release 22).

* $P < .05$ and >2-fold change compared with control.

$ $P < .05$ and <2-fold change compared with control.

# $P < .05$ between chrysotile- and crocidolite-exposed mice (ANOVA followed by Tukey's test, $n = 4$).

TABLE 2 Predicted target genes differentially expressed in lung tissues of asbestos-exposed mice in microarray analysis

Gene	*P*(ANOVA)	Chrysotile (fold vs. control)	Crocidolite (fold vs. control)	Targeted by (predicted)
Pdcd4	.0009	−1.82	−2.03	miR−21
Reck	<.0001	−2.22	−1.52[#]	miR−21
Gdnf	.0004	2.15	1.54[#]	miR−133a
Ppfia3	.0002	2.42	1.61[#]	miR−133a
Fosb	.0001	2.55	1.90	miR−144
Myo1e	<.0001	2.03	1.35[#]	miR−144
Phlda1	.0001	2.86	1.87[#]	miR−144
Lef1	.0001	−3.45	−1.82[#]	miR−449a

Note: These genes were significantly upregulated or downregulated by exposure to chrysotile and crocidolite compared with control ($P < .05$).

Abbreviation: ANOVA, analysis of variance.

[#]$P < .05$, between chrysotile- and crocidolite-exposed mice (ANOVA followed by Tukey's test, $n = 4$).

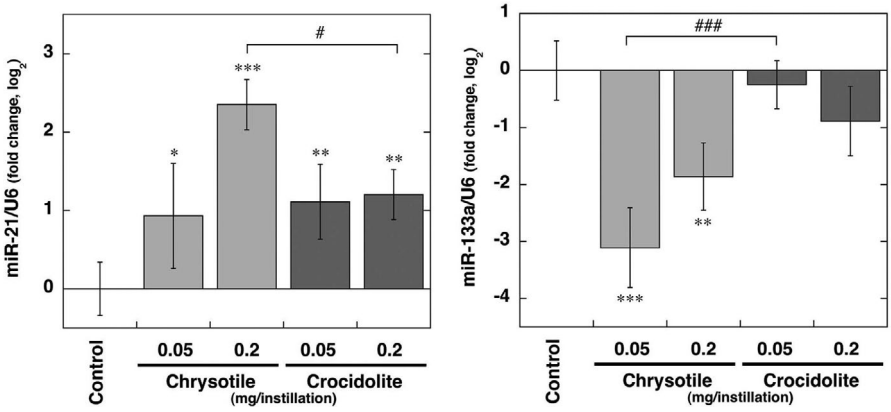

FIGURE 1 miRNA expression in lung tissues of asbestos-exposed mice. The expression levels of miR-21 and miR-133a were quantified by real-time PCR as described in Section 2. U6 snRNA was used as an internal control. Data were expressed as means ± SD of 4–5 independent experiments. *$P < .05$, **$P < .01$, and ***$P < .001$, compared with control; [#]$P < .05$ and [###]$P < .001$, between chrysotile and crocidolite by ANOVA followed by Tukey's test. ANOVA, analysis of variance; miRNA, microRNA; PCR, polymerase chain reaction; SD, standard deviation

participate in tumor development or suppression, and the results are shown in Figure 2A. The expression level of *Pdcd4* was not significantly changed by asbestos exposure, although it tended to be decreased at the high dose of chrysotile. *Reck* was significantly downregulated by both chrysotile and crocidolite at the high dose ($P < .05$). *Gdnf* was significantly upregulated by chrysotile exposure ($P < .001$) but crocidolite did not induce a significant change. There was a significant difference in *Gdnf* expression level between chrysotile- and crocidolite-exposed mice ($P < .05$).

Figure 2B shows the correlation of the expression levels of miRNA and predicted target genes. Although the expression level of miR-21 was not correlated with that of *Pdcd4*, there was a significant negative correlation between the expression levels of miR-21 and *Reck* ($r = -.609$, $P < .01$ by Pearson's correlation test). The expression level of miR-133a was significantly and negatively correlated with that of *Gdnf* ($r = -.595$, $P < .01$). The correlation of expression levels of mRNA and target gene was separately analyzed in chrysotile- and crocidolite-exposed groups (including control in each group). The expression level of miR-21 was not correlated with that of *Pdcd4* in both chrysotile- and crocidolite-exposed mice, but significantly correlated with *Reck* expression in chrysotile- ($r = -.767$, $P < .01$) and crocidolite-exposed mice ($r = -.573$, $P < .05$). The expression level of miR-133a was significantly correlated with that of *Gdnf* in chrysotile-exposed mice ($r = -.678$, $P < .01$) but not in crocidolite-exposed mice ($r = -.096$, $P = .743$).

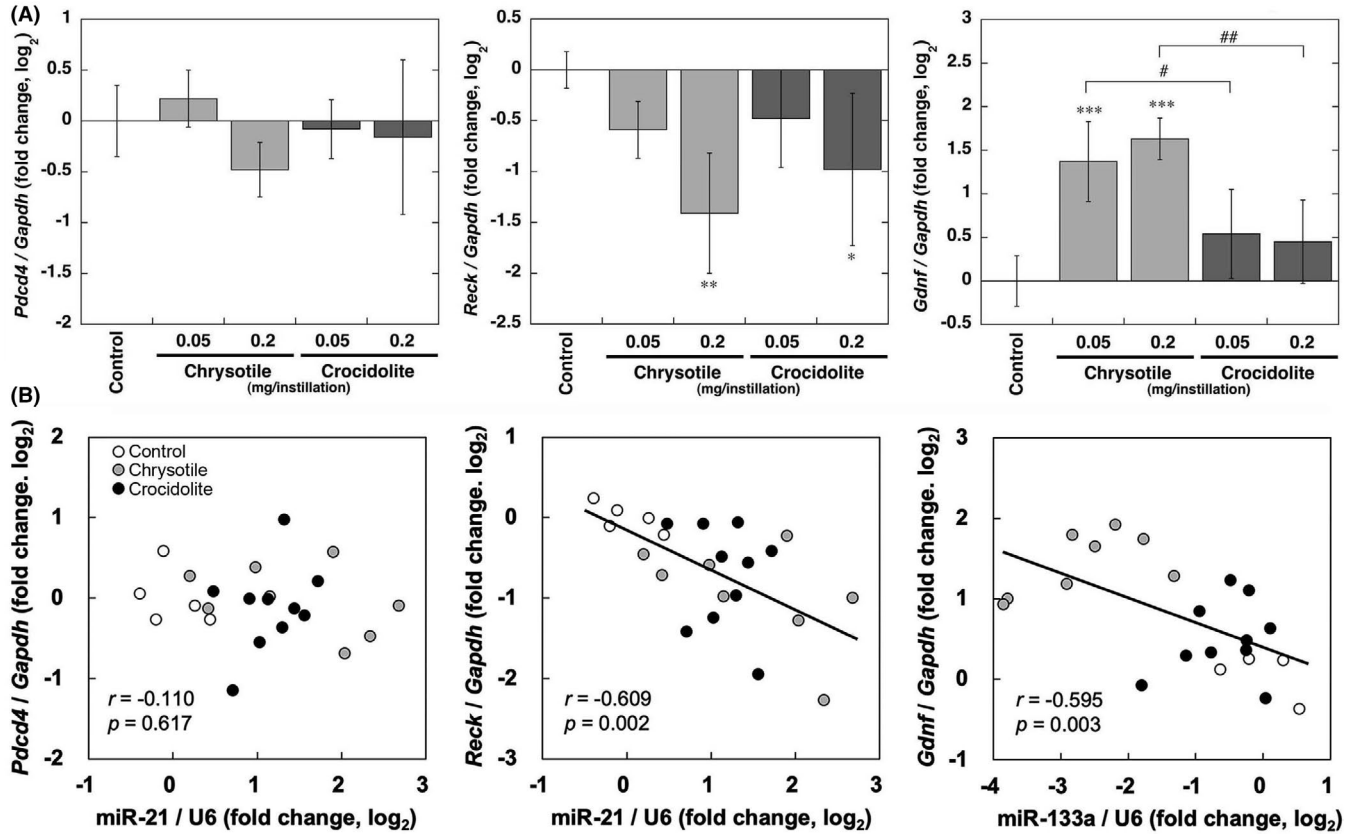

FIGURE 2 Expression of predicted target genes of miRNAs in lung tissues of asbestos-exposed mice and correlation with miRNA expression. (A) Expression of predicted target genes of miR-21 and miR-133a. Expression levels of predicted target genes of miR-21 (*Pdcd4* and *Reck*) and miR-133a (*Gdnf*) were quantified by real-time PCR as described in Section 2. *Gapdh* was used as an internal control. Data were expressed as means ± SD of 4–5 independent experiments. $^{*}P < .05$, $^{**}P < .01$ and $^{***}P < .001$ compared with control; $^{\#}P < .05$ and $^{\#\#}P < .01$, between chrysotile and crocidolite by ANOVA followed by Tukey's test. (B) Correlation of the expression levels of miRNA and predicted target genes. Individual points show the expression levels of mRNA and corresponding target gene in each lung tissue. The correlations of the expression levels of miRNAs and target genes were analyzed by Pearson's correlation test. ANOVA, analysis of variance; miRNA, microRNA; PCR, polymerase chain reaction; PDCD4, programmed cell death 4; RECK, reversion-inducing-cysteine-rich protein with kazal motifs; SD, standard deviation

3.5 | Downregulation of PDCD4 and RECK at the protein level

We examined the downregulation of PDCD4 and RECK at the protein level as potential target genes of miR-21. Western blotting revealed that PDCD4 expression was decreased by asbestos exposure (Figure 3A). Image analysis revealed that chrysotile significantly reduced the intensity of PDCD4 expression ($P < .01$). Crocidolite tended to decrease PDCD4 expression, but not significant ($P = .078$, Figure 3B). There was a significant and negative correlation between the expression levels of miR-21 and PDCD4 ($r = -.860$, $P < .001$, Figure 3C).

Figure 4 shows histopathological changes in lung tissues of asbestos-exposed mice and reduction in PDCD4 and RECK staining evaluated by fluorescent immunohistochemistry. HE and MT staining revealed that chrysotile and crocidolite induced mild pathological changes in lung tissues and no neoplastic lesions were observed (Figure 4A). MT staining showed that asbestos exposure induced no obvious fibrosis, although the slight fibrotic change was observed in the tissue where crocidolite fibers were trapped (Figure 4A). To examine macrophage infiltration, we performed immunoperoxidase staining for CD68, a macrophage marker. In control mice, a few CD68-positive cells were found in alveolar spaces as reported previously.[20] In asbestos-exposed mice, macrophage infiltration was mild but more frequently observed than in control mice. Crocidolite fibers appeared to be phagocytosed by macrophages (Figure 4A).

Fluorescent immunohistochemistry revealed that PDCD4 was positive in most bronchial and alveolar epithelial cells in control mice, and in asbestos-exposed mice, its expression was largely reduced in these cells throughout the lung tissues (Figure 4B). Quantitative image analysis showed that chrysotile and crocidolite

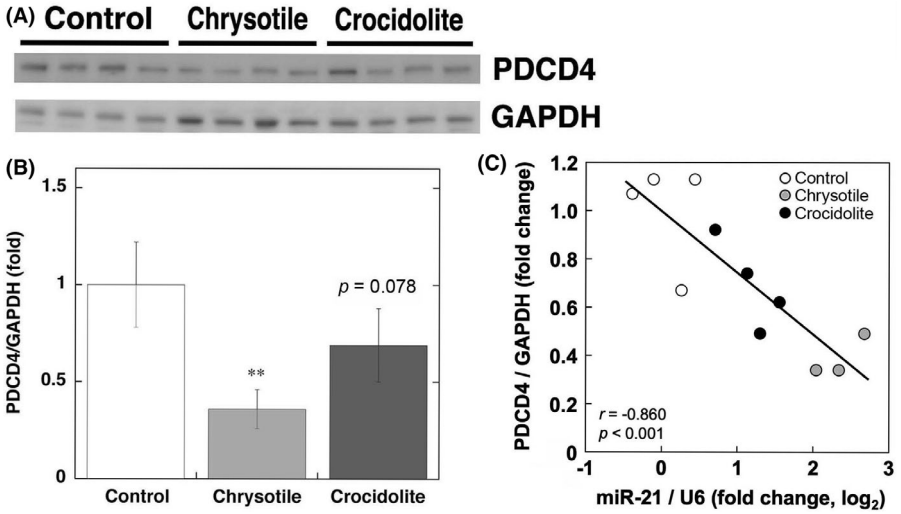

FIGURE 3 PDCD4 expression in lung tissues of asbestos-exposed mice at the protein level. (A) PDCD4 expression in lung tissues evaluated by Western blotting. Western blotting was performed as described in Section 2. (B) Quantitative image analysis of PDCD4 expression. Data were expressed as means ± SD of four independent experiments. $^{**}P < .01$, compared with control by ANOVA followed by Tukey's test. (C) Correlation of the expression levels of miR-21 and PDCD4. miR-21 expression was quantified by real-time PCR as described in Section 2. Individual points show the expression levels of miR-21 and PDCD4 in each lung tissue. The correlation of the expression levels of miR-21 and PDCD4 was analyzed by Pearson's correlation test. ANOVA, analysis of variance; PCR, polymerase chain reaction; PDCD4, programmed cell death 4; SD, standard deviation

significantly and non-significantly reduced the staining intensity of PDCD4 ($P < .01$ and $P = .097$), respectively (Figure 4C). The proportion of PDCD4-positive cells was significantly decreased by both chrysotile ($P < .01$) and crocidolite ($P < .05$, Figure 4D). For RECK expression, fluorescent immunohistochemistry revealed that its expression was also reduced in bronchial and alveolar epithelial cells throughout the lung tissues of asbestos-exposed mice compared with the control mice (Figure 4E). Image analysis showed that chrysotile and crocidolite significantly and non-significantly reduced the staining intensity of RECK ($P < .01$ and $P = .067$), respectively (Figure 4F). The proportion of RECK-positive cells was significantly decreased by chrysotile ($P < .05$), but not crocidolite (Figure 4G).

4 | DISCUSSION

In this study, we performed microarray analysis for miRNA and gene expression in lung tissues of asbestos-exposed mice. We employed a mouse model of subacute asbestos exposure to examine miRNA expression as early response that may lead to carcinogenesis. The expression levels of 14 miRNAs were significantly changed by exposure to chrysotile and/or crocidolite. We predicted target genes of these miRNAs by database analysis. Potential target genes were found for miR-21, miR-133a, miR-144, and miR-449a. Among them, miR-21 was significantly upregulated in the lung tissues of asbestos-exposed mice and predicted to target *Pdcd4* and *Reck* tumor suppressor genes.

FIGURE 4 Histopathological changes and fluorescent immunohistochemical analysis for PDCD4 and RECK in lung tissues of asbestos-exposed mice. (A) Histopathological changes in lung tissues of asbestos-exposed mice. Histopathological changes were examined by HE and MT staining. Macrophage infiltration was examined by immunoperoxidase staining for CD68 as described in Section 2. Black arrows indicate CD68-positive cells. Red arrows in insets (MT and CD68) indicate crocidolite fibers. Scale bar = 100 μm. (B) Fluorescent images for PDCD4 expression in lung tissues of asbestos-exposed mice. Histopathological changes were examined by HE staining. Fluorescent immunohistochemistry was performed as described in Section 2. The nuclei were stained with DAPI. Scale bar = 50 μm. (C) Quantitative image analysis for PDCD4 expression. The staining intensity per field was analyzed with an ImageJ software as described in Section 2. (D) Proportion of PDCD4-positive cells. We calculated the proportion of positive cells as described in Section 2. (E) Fluorescent images for RECK expression. HE staining and fluorescent immunohistochemistry were performed as described in (B). Scale bar = 50 μm. (F) Quantitative image analysis for RECK expression. The staining intensity per field was analyzed as described in (C). (G) Proportion of RECK-positive cells. We calculated the proportion of positive cells as described in (D). (C, D, F, G) Data were expressed as means ± SD of three independent experiments. $^{*}P < .05$ and $^{**}P < .01$, compared with control by ANOVA followed by Tukey's test. ANOVA, analysis of variance; DAPI, 4′,6-diamidino-2-phenylindole; HE, hematoxylin and eosin; MT, Masson's trichrome; PDCD4, programmed cell death 4; RECK, reversion-inducing-cysteine-rich protein with kazal motifs; SD, standard deviation

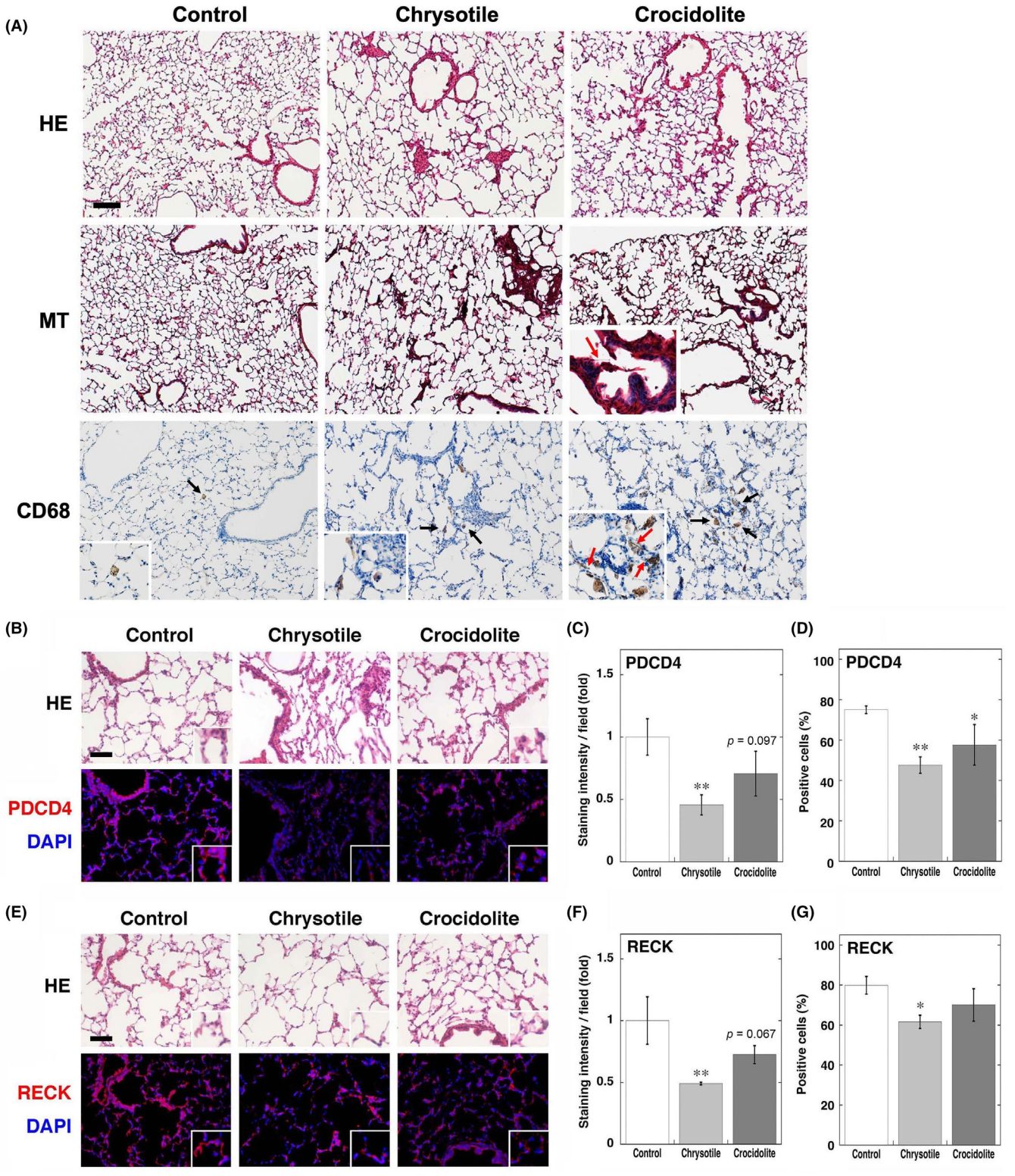

A previous study showed that miR-21 was overexpressed in non-small cell lung cancer tissues compared with non-tumor tissues.[21] Meta-analysis of miRNA expression studies in human lung cancer tissues revealed that miR-21 was significantly upregulated in cancer tissues compared with non-cancerous tissues.[14] The plasma expression level of miR-21 was higher in patients with lung cancer than in healthy controls.[22] miR-21 overexpression in cancer tissues and serum was associated with poor prognosis of lung cancer patients.[23,24] In association with asbestos exposure, miR-21 expression was related to histological subtypes in malignant mesothelioma patients.[9] The molecular link between miR-21 and PDCD4 was firstly reported in colorectal cell lines and human

colon cancer tissues.[15] Downregulation of miR-21 expression restrains lung cancer cell proliferation and migration through PDCD4 upregulation.[25] PDCD4 suppresses tumor transformation by inhibiting activation of the transcription factor AP-1.[26] PDCD4 protein expression was widely lost in human lung cancer samples and the loss of its expression was associated with poor prognosis.[27] miR-21 was also reported to target RECK, an inhibitor of matrix metalloproteinase (MMP), to promote glioma invasion in animal models and human brain tissues.[16] RECK is also negatively regulated by miR-21 in lung squamous carcinoma tissues.[28] RECK interacts with MMP-9 to inhibit the degradation of the extracellular matrix and suppress tumor invasion and metastasis.[29] Downregulation of RECK is associated with poor prognosis of lung cancer patients.[30] The association of miRNA expression with lung cancer has not well been investigated in experimental animals, although a recent study has shown that miR-199 and miR-214 are overexpressed in asbestos-induced sarcomatoid mesothelioma of rats.[13] A recent epidemiological study has reported that serum miR-126 and miR-222 expression is increased in patients with asbestos-induced non-small cell lung cancer compared with disease-free subjects.[31] This is the first study showing that miR-21 was upregulated and its potential target genes PDCD4 and RECK were downregulated in lung tissues of asbestos-exposed animals, raising a possibility that these molecules participate in asbestos-induced lung carcinogenesis.

In this study, although real-time PCR showed that mRNA expression of *Pdcd4* gene was not significantly decreased by asbestos exposure, Western blotting, and immunohistochemistry revealed that PDCD4 expression was reduced by asbestos, especially chrysotile. miRNA directly binds to a target mRNA, resulting in mRNA degradation or inhibition of protein translation.[32] Our results suggest that miR-21 affects the translation process of PDCD4 rather than mRNA degradation. This finding is supported by previous studies showing that the transfection of an antisense oligonucleotide for miR-21 into human embryonic kidney cells and head and neck cancer cells significantly increased the protein level of PDCD4, but did not change its mRNA level.[33,34] Recent studies have demonstrated that chromium and arsenic-induced miR-21 upregulation and PDCD4 downregulation in a lung bronchial cell line, and this pathway appears to be involved in tumor development.[35,36] These findings raise a possibility that miR-21 upregulation and the resulting downregulation of tumor suppressor genes, including *Pdcd4* and *Reck*, contributes to lung carcinogenesis induced by inhalation exposure to industrial chemicals.

Previous studies examined histopathological changes in lung tissues of mice with intratracheal exposure to crocidolite. Long fibers (>20 μm) were deposited in bronchiolar regions and induced fibrosis and granuloma formation, whereas short fibers (<1 μm) reached alveoli but did not induce fibrosis.[37] In this study, we used relatively short asbestos fibers, which induced only mild histopathological changes and macrophage infiltration. A recent study using miR-21 knockout mice has demonstrated that miR-21 plays a critical role in nickel nanoparticle-induced pulmonary inflammation and fibrosis,[38] suggesting that miR-21 precedes asbestos-induced histopathological changes. In this study, fluorescent immunohistochemistry showed that PDCD4 and RECK expression was reduced in bronchial and alveolar cells throughout the lung tissues, even where no histopathological changes occurred. These results imply that these molecular events precede histopathological changes caused by asbestos exposure.

Oxidative and nitrative stress is considered to contribute to asbestos-induced carcinogenesis.[3–5] Several studies have shown that reactive oxygen species (ROS) and reactive nitrogen species (RNS) mediate miR-21 expression in various experimental systems. There are some reports showing that ROS initiate miR-21 expression.[36] Growth factors (epidermal growth factor and basic fibroblast growth factor) induce miR-21 expression and PDCD4 suppression via ROS generation in colon cancer cells.[39] In knockout mice for inducible nitric oxide synthase showed a reduction in miR-21 expression and tumor cell proliferation in KRAS-induced lung carcinogenesis.[40] In this study, chrysotile tended to induce miR-21 upregulation and PDCD4 and RECK downregulation to a greater extent than crocidolite, whereas our previous study showed that crocidolite induced stronger DNA damage mediated by ROS and RNS in lung tissues of mice.[4] Therefore, it is speculated that miR-21 upregulation in this study was not solely accounted for by these reactive species.

We have also observed that miR-133a was significantly downregulated in lung tissues of chrysotile-exposed mice compared with control mice. Clinical studies showed that miR-133a was downregulated in lung cancer tissues compared with corresponding non-tumor tissues.[41–43] miR-133a expression in cancer tissues was negatively associated with clinical stage, metastasis and survival of the patients.[41,43] The transfection of miR-133a significantly reduced the proliferation of lung cancer cell lines.[42] We predicted that miR-133a targets the tumor suppressor gene *Gdnf*. GDNF is a ligand for the RET oncogene product, transduces signals for cell growth and differentiation. GDNF is overexpressed in squamous non-small-cell lung carcinoma, but normally absent in adult lung tissues.[44] Reduction in miR-133a expression and resulting GDNF upregulation may also contribute to asbestos-induced carcinogenesis.

Asbestos includes several types of mineral fibers, such as chrysotile and crocidolite, and carcinogenic potential of each type of asbestos is under debate. Cohort studies of asbestos-exposed workers demonstrated that crocidolite was more potent for causing mesothelioma than chrysotile.[45] In contrast, Jiang et al. have demonstrated that chrysotile caused earlier mesothelioma development with a high fraction of sarcomatoid histology in the rat peritoneal cavity than crocidolite and amosite.[46] In this study, chrysotile tended to induce a more significant change in miRNA expression than crocidolite. This result raises a speculation that the alteration in miRNA expression predominantly contributes to chrysotile-induced carcinogenesis. However, in this study, we used a subacute model of asbestos exposure and cannot exclude the possibility that altered miRNA expression was consequential to fiber exposure. Extensive studies have been conducted to examine molecular events and histopathological changes in mice exposed to particulate matters, including asbestos.[37,38] However, it has been reported that intratracheal administration of asbestos induces lung tumor in rats and hamsters, but not in mice.[1] Although we employed a mouse model with subacute asbestos exposure in this study, further studies using different animal species with long-term asbestos exposure are needed to understand the role of miRNA and target genes in the pathogenesis of asbestos-induced diseases. In addition, further investigation using human specimens is necessary to utilize miRNAs and their target genes as biomarkers to evaluate the risk of these diseases.

ACKNOWLEDGMENTS

This work was supported by Grants-in-Aid for Scientific Research from the Ministry of Education, Culture, Sports, Science and Technology, Japan (Grant numbers 23659328, 24390153, 15H04784 and 18H03038).

AUTHORS' CONTRIBUTIONS

Yusuke Hiraku conceived an idea and designed this study. Takamichi Ichinose performed an animal experiment. Yusuke Hiraku performed microarray and database analysis. Yusuke Hiraku, Jun Watanabe, and Akira Kaneko carried out real-time PCR, Western blotting, and immunohistochemistry. The draft manuscript was written by Yusuke Hiraku and revised critically by Mariko Murata. All authors read, corrected and approved the final manuscript.

DISCLOSURE

Approval of the research protocol: The animal care method was approved by the Animal Care and Use Committee at Oita University of Nursing and Health Sciences in Oita. *Informed consent*: N/A. *Registry and the Registration No. of the study/trial*: N/A. *Animal studies*: The experiment was performed in accordance with Guidelines at Oita University of Nursing and Health Sciences in Oita. *Conflict of interest*: The authors declare that they have no conflicts of interest.

DATA AVAILABILITY STATEMENT

Research data are not shared.

ORCID

Yusuke Hiraku https://orcid.org/0000-0002-4351-1498

REFERENCES

1. IARC. Asbestos (chrysotile, amosite, crocidolite, tremolite, actinolite, and anthophyllite). IARC Monographs on the Evaluation of Carcinogenic Risks to Humans, vol. 100, A Review of Human Carcinogens Part C: Arsenic, Metals, Fibres, and Dusts. Vol 100C.2012:219-309.
2. USGS. Asbestos. In: *Mineral Commodity Summaries 2019*. U.S. Geological Survey; 2019:26-27.
3. Robinson BW, Lake RA. Advances in malignant mesothelioma. *N Engl J Med*. 2005;353(15):1591-1603.
4. Hiraku Y, Kawanishi S, Ichinose T, Murata M. The role of iNOS-mediated DNA damage in infection- and asbestos-induced carcinogenesis. *Ann NY Acad Sci*. 2010;1203:15-22.
5. Hiraku Y, Sakai K, Shibata E, et al. Formation of the nitrative DNA lesion 8-nitroguanine is associated with asbestos contents in human lung tissues: a pilot study. *J Occup Health*. 2014;56(3):186-196.
6. Bayoumi AS, Sayed A, Broskova Z, et al. Crosstalk between long noncoding RNAs and microRNAs in health and disease. *Int J Mol Sci*. 2016;17(3):356.
7. Chen Z, Gaudino G, Pass HI, Carbone M, Yang H. Diagnostic and prognostic biomarkers for malignant mesothelioma: an update. *Transl Lung Cancer Res*. 2017;6(3):259-269.
8. Guled M, Lahti L, Lindholm PM, et al. CDKN2A, NF2, and JUN are dysregulated among other genes by miRNAs in malignant mesothelioma-A miRNA microarray analysis. *Genes Chromosomes Cancer*. 2009;48:615-623.
9. Busacca S, Germano S, De Cecco L, et al. MicroRNA signature of malignant mesothelioma with potential diagnostic and prognostic implications. *Am J Resp Cell Mol Biol*. 2010;42(3):312-319.
10. Kirschner MB, Cheng YY, Badrian B, et al. Increased circulating miR-625-3p: a potential biomarker for patients with malignant pleural mesothelioma. *J Thorac Oncol*. 2012;7(7):1184-1191.
11. Weber DG, Gawrych K, Casjens S, et al. Circulating miR-132-3p as a candidate diagnostic biomarker for malignant mesothelioma. *Dis Markers*. 2017;2017:9280170.
12. Mozzoni P, Ampollini L, Goldoni M, et al. MicroRNA expression in malignant pleural mesothelioma and asbestosis: a pilot study. *Dis Markers*. 2017;2017:9645940.
13. Okazaki Y, Chew SH, Nagai H, et al. Overexpression of miR-199/214 is a distinctive feature of iron-induced and asbestos-induced sarcomatoid mesothelioma in rats. *Cancer Sci*. 2020;111(6):2016-2027.
14. Vosa U, Vooder T, Kolde R, Vilo J, Metspalu A, Annilo T. Meta-analysis of microRNA expression in lung cancer. *Int J Cancer*. 2013;132(12):2884-2893.
15. Asangani IA, Rasheed SA, Nikolova DA, et al. MicroRNA-21 (miR-21) post-transcriptionally downregulates tumor

suppressor Pdcd4 and stimulates invasion, intravasation and metastasis in colorectal cancer. *Oncogene*. 2008;27(15):2128-2136.
16. Gabriely G, Wurdinger T, Kesari S, et al. MicroRNA 21 promotes glioma invasion by targeting matrix metalloproteinase regulators. *Mol Cell Biol*. 2008;28(17):5369-5380.
17. Kohyama N, Shinohara Y, Suzuki Y. Mineral phases and some reexamined characteristics of the International Union Against Cancer standard asbestos samples. *Am J Ind Med*. 1996;30(5):515-528.
18. Saito R, Hirakawa S, Ohara H, et al. Nickel differentially regulates NFAT and NF-κB activation in T cell signaling. *Toxicol Appl Pharmacol*. 2011;254(3):245-255.
19. Hiraku Y, Guo F, Ma N, et al. Multi-walled carbon nanotube induces nitrative DNA damage in human lung epithelial cells via HMGB1-RAGE interaction and Toll-like receptor 9 activation. *Part Fibre Toxicol*. 2016;13(1):16.
20. Schyns J, Bai Q, Ruscitti C, et al. Non-classical tissue monocytes and two functionally distinct populations of interstitial macrophages populate the mouse lung. *Nat Commun*. 2019;10(1):3964.
21. Liu ZL, Wang H, Liu J, Wang ZX. MicroRNA-21 (miR-21) expression promotes growth, metastasis, and chemo- or radioresistance in non-small cell lung cancer cells by targeting PTEN. *Mol Cell Biochem*. 2013;372(1-2):35-45.
22. Tang D, Shen Y, Wang M, et al. Identification of plasma microRNAs as novel noninvasive biomarkers for early detection of lung cancer. *Eur J Cancer Prev*. 2013;22(6):540-548.
23. Gao W, Shen H, Liu L, Xu J, Xu J, Shu Y. miR-21 overexpression in human primary squamous cell lung carcinoma is associated with poor patient prognosis. *J Cancer Res Clin Oncol*. 2011;137(4):557-566.
24. Liu XG, Zhu WY, Huang YY, et al. High expression of serum miR-21 and tumor miR-200c associated with poor prognosis in patients with lung cancer. *Med Oncol*. 2012;29(2):618-626.
25. Yang Y, Meng H, Peng Q, et al. Downregulation of microRNA-21 expression restrains non-small cell lung cancer cell proliferation and migration through upregulation of programmed cell death 4. *Cancer Gene Ther*. 2015;22(1):23-29.
26. Yang HS, Jansen AP, Nair R, et al. A novel transformation suppressor, Pdcd4, inhibits AP-1 transactivation but not NF-κB or ODC transactivation. *Oncogene*. 2001;20(6):669-676.
27. Chen Y, Knosel T, Kristiansen G, et al. Loss of PDCD4 expression in human lung cancer correlates with tumour progression and prognosis. *J Pathol*. 2003;200(5):640-646.
28. Xu LF, Wu ZP, Chen Y, Zhu QS, Hamidi S, Navab R. MicroRNA-21 (miR-21) regulates cellular proliferation, invasion, migration, and apoptosis by targeting PTEN, RECK and Bcl-2 in lung squamous carcinoma, Gejiu City, China. *PLoS One*. 2014;9(8):e103698.
29. Takahashi C, Sheng Z, Horan TP, et al. Regulation of matrix metalloproteinase-9 and inhibition of tumor invasion by the membrane-anchored glycoprotein RECK. *Proc Natl Acad Sci USA*. 1998;95(22):13221-13226.
30. Takenaka K, Ishikawa S, Kawano Y, et al. Expression of a novel matrix metalloproteinase regulator, RECK, and its clinical significance in resected non-small cell lung cancer. *Eur J Cancer*. 2004;40(10):1617-1623.
31. Santarelli L, Gaetani S, Monaco F, et al. Four-miRNA signature to identify asbestos-related lung malignancies. *Cancer Epidemiol Biomarkers Prev*. 2019;28(1):119-126.
32. Nana-Sinkam SP, Hunter MG, Nuovo GJ, et al. Integrating the MicroRNome into the study of lung disease. *Am J Respir Crit Care Med*. 2009;179(1):4-10.
33. Lu Z, Liu M, Stribinskis V, et al. MicroRNA-21 promotes cell transformation by targeting the programmed cell death 4 gene. *Oncogene*. 2008;27(31):4373-4379.
34. Sun Z, Li S, Kaufmann AM, Albers AE. miR-21 increases the programmed cell death 4 gene-regulated cell proliferation in head and neck squamous carcinoma cell lines. *Oncol Rep*. 2014;32(5):2283-2289.
35. Pratheeshkumar P, Son YO, Divya SP, Wang L, Zhang Z, Shi X. Oncogenic transformation of human lung bronchial epithelial cells induced by arsenic involves ROS-dependent activation of STAT3-miR-21-PDCD4 mechanism. *Sci Rep*. 2016;6:37227.
36. Pratheeshkumar P, Son YO, Divya SP, et al. Hexavalent chromium induces malignant transformation of human lung bronchial epithelial cells via ROS-dependent activation of miR-21-PDCD4 signaling. *Oncotarget*. 2016;7(32):51193-51210.
37. Adamson IY, Bakowska J, Bowden DH. Mesothelial cell proliferation after instillation of long or short asbestos fibers into mouse lung. *Am J Pathol*. 1993;142(4):1209-1216.
38. Mo Y, Zhang Y, Wan R, Jiang M, Xu Y, Zhang Q. miR-21 mediates nickel nanoparticle-induced pulmonary injury and fibrosis. *Nanotoxicology*. 2020;14(9):1175-1197.
39. Saxena A, Shoeb M, Ramana KV, Srivastava SK. Aldose reductase inhibition suppresses colon cancer cell viability by modulating microRNA-21 mediated programmed cell death 4 (PDCD4) expression. *Eur J Cancer*. 2013;49(15):3311-3319.
40. Okayama H, Saito M, Oue N, et al. NOS2 enhances KRAS-induced lung carcinogenesis, inflammation and microRNA-21 expression. *Int J Cancer*. 2013;132(1):9-18.
41. Wang Y, Li J, Chen H, et al. Down-regulation of miR-133a as a poor prognosticator in non-small cell lung cancer. *Gene*. 2016;591(2):333-337.
42. Moriya Y, Nohata N, Kinoshita T, et al. Tumor suppressive microRNA-133a regulates novel molecular networks in lung squamous cell carcinoma. *J Hum Genet*. 2012;57(1):38-45.
43. Lan D, Zhang X, He R, et al. MiR-133a is downregulated in non-small cell lung cancer: a study of clinical significance. *Eur J Med Res*. 2015;20:50.
44. Garnis C, Davies JJ, Buys TP, et al. Chromosome 5p aberrations are early events in lung cancer: implication of glial cell line-derived neurotrophic factor in disease progression. *Oncogene*. 2005;24(30):4806-4812.
45. Garabrant DH, Pastula ST. A comparison of asbestos fiber potency and elongate mineral particle (EMP) potency for mesothelioma in humans. *Toxicol Appl Pharmacol*. 2018;361:127-136.
46. Jiang L, Akatsuka S, Nagai H, et al. Iron overload signature in chrysotile-induced malignant mesothelioma. *J Pathol*. 2012;228(3):366-377.

How to cite this article: Hiraku Y, Watanabe J, Kaneko A, Ichinose T, Murata M. MicroRNA expression in lung tissues of asbestos-exposed mice: Upregulation of miR-21 and downregulation of tumor suppressor genes *Pdcd4* and *Reckt*. *J Occup Health*. 2021;63:e12282. https://doi.org/10.1002/1348-9585.12282